LAND-WATER MASKS: BASIS FOR AUTOMATED PRE- AND THEMATIC PROCESSING OF REMOTE SENSING DATA

Erik Borg, Bernd Fichtelmann

ABSTRACT

Earth observation data have become an outstanding basis for analyzing environmental aspects. The increasing availability of remote sensing data is accompanied by an increasing user demand. Within the scope of the COOPERNICUS-initiative, the automatic processing of remote sensing data is important for supplying value-added-information products. The use of additional data like land-water-masks in the context of deriving value-added information products can stabilize and improve the product quality of information products.

The authors of this contribution would like to discuss different automated processing algorithms which are based on land-water masks for value-added data interpretation. These developments were supported or accompanied by Prof. Hartmut Asche.

1 INTRODUCTION

Started in 2003 the Global Monitoring for Environment and Security (GMES) program is a political initiative to secure Europe with an autonomous and operational information production system in support to environment and security policies co-lead by the European Commission (EC) and the European Space Agency (ESA) (http://www.eurogeographics.org/sites/default/files/imported-files/documents/GMES_Newsletter_1.pdf). This initiative is aimed at the development and provision of substantial, accurate and stable geo-information services based on remote sensing data products and ancillary spatial data, e.g. in-situ-information. For that purpose, a range of current remote sensing technologies, including radar and multi-satellite systems, have been employed to establish a geographical database on environmental information. Many of the environmental parameters required can be detected by optical remote sensing systems only. In 2014, The European Parliament (EP) adopted the European Earth Observation program COPERNICUS to establish an European geo-information market for different environmental, economic, and safety-relevant aspects. In addition innovative information products and services using satellite-based remote sensing data are to be developed.

To supply stable and continuous services, satellite systems as well as ground segments (e.g. receiving stations), the near-real- and real-time processing of remote sensing data (automatic basis processors like e.g. geo-, atmosphere correction) are needed. The inclusion of additional sources of information (e.g. in-situ-monitoring networks) and the development of data assimilation models (e.g. biomass and erosion models) are necessary to derive sophisticated spatial information products fitted to the need of the user.

While the development of the satellite-supported space segment and ground segment has progressed forward, the development of automated processing algorithms and processing chains must be forced in order to deliver value added information products in for the user acceptable quantity, quality, and time.

The present trend in data acquisition by earth observation is forced by increasing requirements for actual and full-coverage information about state, change and development of the environment. This information is a substantial basis for understanding complex environmental systems with respect of decision and action scenarios. Realistic scenarios need quantitative information products combined with accuracy assessment.

Therefore proofed and reliable algorithms for deriving information products are needed for automatic processing systems.

The challenges for the development of automated, operational processors of remote sensing data are the great number of processing steps as e.g.

» *calibration of sensor data,*
» *geometric correction,*
» *pre-classification of water, snow, ice, cloud and cloud shadow, atmospheric correction including topographic shadow correction and probably BRDF correction, and*
» *finally the derivation of thematic parameter (e.g. leaf area index, land classification).*

The accuracy of each individual processing step should be assessed and included in the final product. But in many cases the automated thematic processing of remote sensing data is performed using pre-processed data
» *missing some of the above mentioned steps or*
» *showing inaccuracies with regard to the above mentioned steps.*

Therefore, the thematic product can show low accuracy with regard to e.g. the geo-location of each pixel, false pre-classification or inappropriate atmospheric correction.

In this overview we will demonstrate the improvement of remote sensing products applying static and dynamic land-water masks in automatic processing chains. Therefore, we give a short view how thematic products (e.g. quick look product "Chlorophyll Concentration in the Baltic Sea") can be improved using land-water masks or the generation of a static land-water mask as additional decision criterion for data quality assessment. Second, we show the way how to classify water areas in geo-located, calibrated optical remote sensing data using a dynamic approach. Finally, we show how the geo-location can be improved for Landsat data using land-water masks.

2 AVAILABLE STATIC LAND-WATER MASKS

In our investigations the generation of a consistent global static land-water mask is based on the following data: CIA World-Map (Pape, last modified 2004), used in the first studies “Chlorophyll Concentration in the Baltic Sea” for generation of the quick look NRT (Near Real Time) product (Krawczyk et al., 1995) or data quality assessment of LANDSAT 7 data (Borg, 2007; Borg et al. 2012), than substituted by SRTM Water Body Data (SWDB; USGS, 2003), and GSHHS, released in 2011 (Wessel and Smith, 1996). Actually static land-water masks can be used to derive the fraction of water area for each data pixel in percentage if the resolution of image data is lower than the data of mask. The generation of a consistent static land-water mask is described in Fichtelmann et al., 2011 in more detail. For quality checks of our dynamic land-water masks we used additionally the Global Lakes and Wetlands Database (GLWD) (Lehner and Doell, 2004) and the Global 250 m Land Water Mask (MOD44W) (Carroll et al., 2009) as already described in Fichtelmann et al. (2014).

The supply of global information products increased in the last years. Examples for this statement are e.g. Hansen, 2013a and b. The quality of this land-water mask (Hansen_GFC) was examined against the SRTM mask for a selected region (Fichtelmann et al., 2015). Beside of small changes in the shoreline of lakes some smaller water bodies are included and also small islands in lakes. The main advantage consists in the fact that in contrast to the SRTM mask the high quality is also available beyond 60° N. The progress in development and use of such masks is primarily driven by e.g. the increasing availability of free remote sensing data (e.g. LANDSAT, SENTINEL).

Especially in the context of automated processing of remote sensing data, the inclusion of additional data in the value-adding process of remote sensing data gained importance in the past (Fichtelmann et al., 2011). A class of this global available thematic information layer is the group of the land water masks. In Table 1a number of free available land-water masks with their spatial characteristics are shown. These data can be integrated as additional information in the pre- and thematic processing of the value-adding of remote sensing data.

Land-Water-Mask	Data Basis	Region	Distribution size	Spatial Resolution
CIA World Data Bank II, created by the U.S. government in the 1980s	CIA World Data Bank II	Global	5 data files: Africa, Europe, Asia, North- and South America	< 100 m
SWBD (USGS, 2003)	SRTM	180° W - 180° E and between 60° S and 60° N	1 x 1 degree	< 30 m
GSHHS released in 2011 (Wessel and Smith, 1996)	CIA World Data Bank II, World Vector Shorelines	Global, lakes > 1 km used in fire_cci: region 60° N to 90° N	10 x 10 degrees	< 100 m
RANGS (Regionally Accessible Nested Global Shorelines) (Feistel, 1999)	GSHHS	Global	1 x 1 degree (developed to overcome disadvantages in use of GSHHS cells)	< 100 m
GLWD (Global Lakes and Wetlands Database) (Lehner and Doell, 2004)	masks of different sources	Global	3 layers: 1. polygons of 3067 lakes (area $\geq$ 50 km^2) + 654 reservoirs (storage capacity $\geq$ 0.5 km^3) worldwide 10 m, 2. polygons of lakes (area $\geq$ 0.1 km^2), 3. Global raster map: resolution 30“	30 m
MOD44W (Carroll et al., 2009)	SWBD, MODIS 250 m, mosaic of Antarctica	Global	(16-20) x 12 degrees	250 m
Hansen_GFC (Hansen et al., 2013, a and b)	LANDSAT 7	180° W - 180° E and between 80° N - 60° S	10 x 10 degrees	30 m
GIW 2000 (Feng et al., 2015)	LANDSAT 7	Global	global notation system for Landsat data with path and row, 8756 subsets	30 m

Table 1: Different free available land-water masks with their specifics are listed (Lehner and Doell, 2004, modified and complemented by Borg et al., 2016).

3 THE USE OF STATIC LAND-WATER MASK AS ADDITIONAL DATA IN AUTOMATIC PROCESSING

3.1 Monitoring of the chlorophyll concentration

An example for an automated quick look processor “Chlorophyll Concentration in the Baltic Sea” is given in the following. The thematic product is based on the data of the space borne imaging spectrometer Modular Optoelectronic Scanner (MOS) on board of the Indian Remote Sensing Satellite IRS-P3 (launched on March 21st 1996). The automatic processing chain was started in 1998. The aim was the production of results directly after data receiving (Near Real Time) and their publication via Internet as well as appropriate users (Wolff et al., 1998). Figure 1c shows an example of such a delivered product. The typical situation of the chlorophyll concentration in the Baltic Sea looks reasonable (low concentration in the northern part and higher concentration south of Sweden) as well as the range of concentration.

Figure 1a and b show the CIA land-water mask for the Baltic region. Its use in generation of quick-look-products would deliver inconsistent information products. The deficits shown in figure 1 a and b were resulting from missing information “water” for lakes, “land” for islands, and an unprecise water distribution along the coast line of the Baltic Sea.

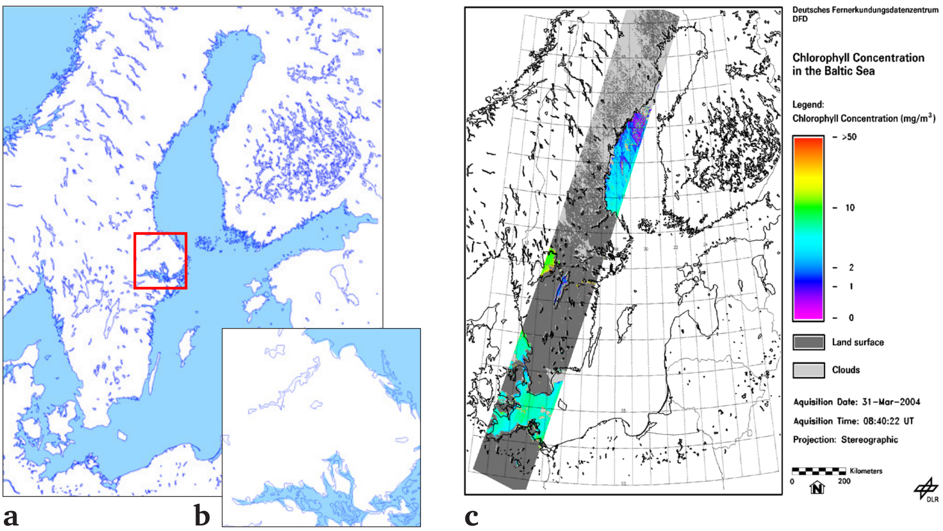

Figure 1: Precise land-water-mask (a). The section shows details of the map around Stockholm (b). Quick-look product of a MAPP product based on MERIS data (with kind permission of Birgit Gerasch) (c).

Therefore, the shown application is a sample for only using the shoreline information of the CIA world map data (available in IDL software) and the corresponding land-water distribution was not used. The information "land surface" marked with dark grey is based on the classification algorithm applied to the MOS data.

The further product development in the context of the "MERIS Application and Regional Products Project" (MAPP, funded by the BMBF) was aimed at making land-water information available for products of higher quality. Efforts have been made to eliminate the listed deficits above (Krawczyk and Neumann, 2010). Figure 2c demonstrates an example of a chlorophyll product which is based on a land-water-mask (Figure 2a).

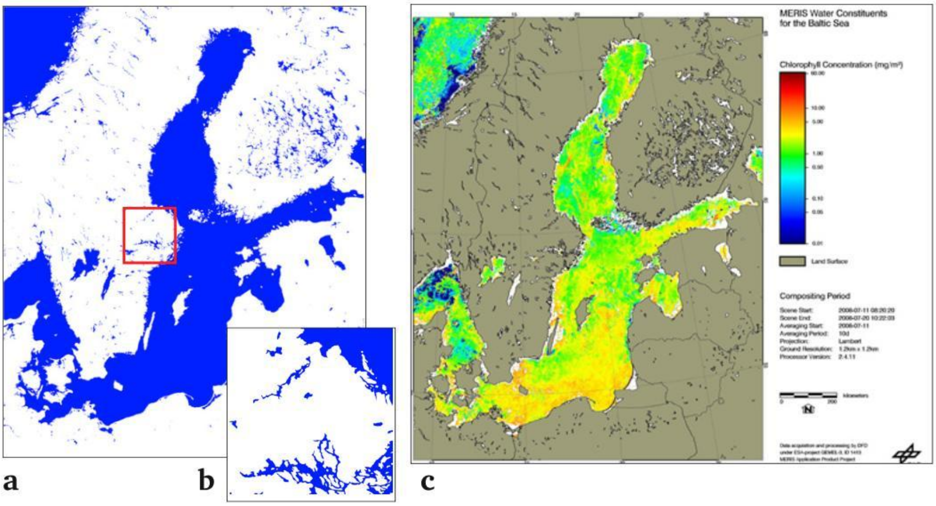

Figure 2: Land-water-mask of limited quality (a). The section shows details of the map around Stockholm (b). Quick-look product "Chlorophyll Concentration in the Baltic Sea" based on MOS data (c).

The resulting static land-water can be seen in Figure 2a and b. The static land pixels are marked with gray colour (Figure 2c). Masks are also produced for further MAPP product regions like North Sea, Europe and Lake Constance.

3.2 Complementary Data for the Data Usability Assessment

The interactive processing of remote sensing data is time consuming and cost expensive. Therefore interactive evaluation can only concentrate upon unclouded to in maximum moderately clouded data. The analysis of all available data (e.g. time series) requires the development and application of automatic processors and operational processing chains.

But for interactive as well as automatic data processing an exact knowledge of the data quality is important. The quality parameter of optical remote sensing data can directly be derived from a given dataset. It can either be expressed in terms of the cloud cover index or the data usability index. The data usability processor for LANDSAT 7/ETM+ optical remote sensing data (Borg et al., 2013) can be integrated in an automated value added processing chain.

By applying an algorithm for transforming land-water masks into satellite-projection by using the corner coordinates an additional information layer with land-water information is added to the remote sensing data so that: i) the sensitivity of a haze-cloud detection algorithm can be controlled according to the underlying class "land" or "water" and ii) the data quality assessment can be controlled according to the land-water distribution.

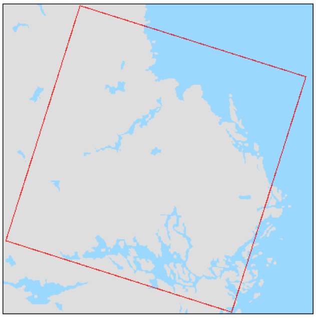

Figure 3: Sample of an automated generation of map with land-water mask for Landsat 7 ETM+ -data on basis of the available corner coordinates of metadata.

Based on CIA World map data (available in IDL) and a map generation algorithm we generate for each remote sensing data set a land-water mask (Figure 3) and finally, by using an inverse geo-rectification a land-water mask as additional layer to the image data. The computed water-mask is shown on top left of the quality assessment product (Figure 4). Beside the information to the data set, the quick-look representation on the right site, the geographical information about the received pass, the processed scenes and the scene immediately in the processing on the bottom left, the information about the data quality (data usability) is shown for the four assessment segments. The cloud mask is plotted on the suitable RGB-representation of the scene. Beside this, the processing time of 27 seconds required for computing of the scene is shown.

In principle, the procedure which was developed for the fast automatic quality assessment of Landsat-data can be applied for other data. For this, the algorithm as well as the surface for presenting and control of the results were generalized, while, e.g., a varying data size, like with ALOS with tilteable sensor, was implemented.

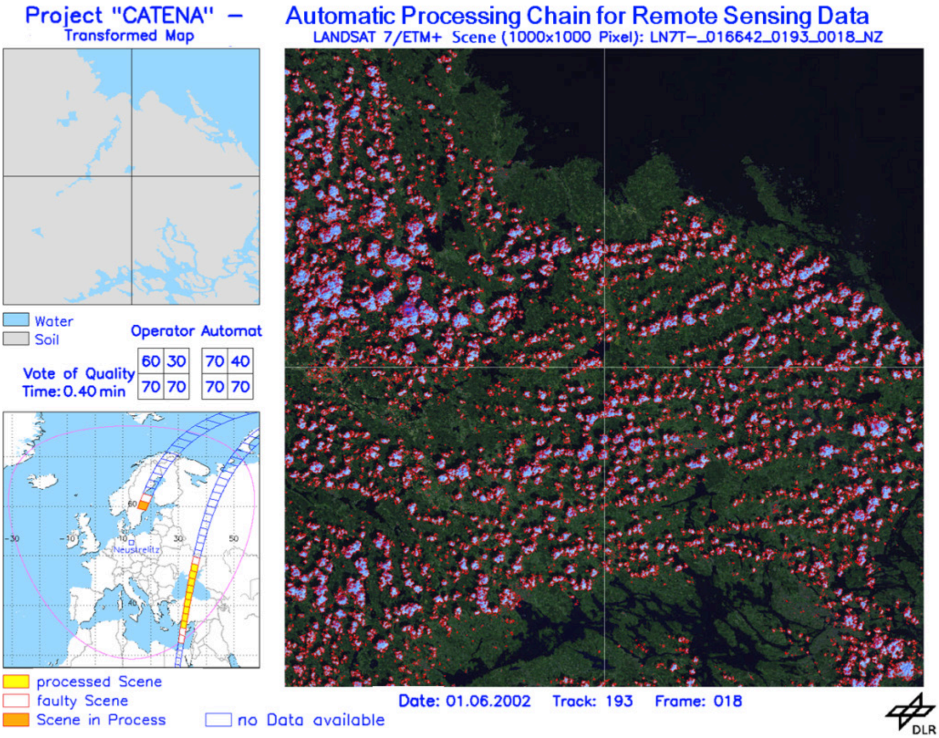

Figure 4: Sample of a result of an automated cloud detection and data usability assessment for Landsat 7 ETM+ -data. The static land-water mask in the upper left shows the result of inverse geo-rectification of the region covered by a Landsat data set in the region of Stockholm shown in Figure 3.

3.3 Improving geo-location applying land-water masks

A further example of the use of land water masks for pre-processing of remote sensing data is the geo-referencing. In principle there exist a number of different geo-referencing methods. A survey of available technologies is given by (Brown, 1992, Zitova & Flusser, 2003, Toutin, 2004, Saxena & Singh, 2014). One of these proposed technologies is the feature-based matching or geo-referencing method (Li, 1988). A precondition for this method is a reference basis like an ortho- or geo-rectified map

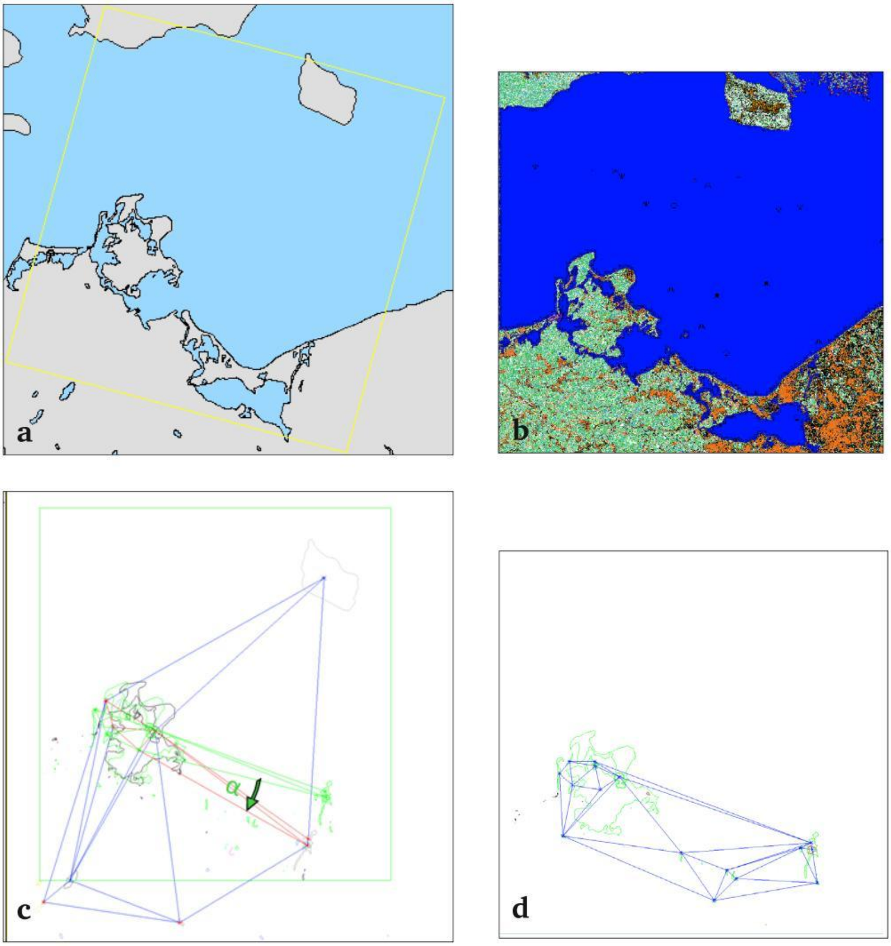

Figure 5: Geo-referencing of classified LANDSAT 7 quick-look (b) based on CIA land-water mask (a). The contours of usable objects, centroids and graph network (blue) are shown in c) and d). In c) is added the graph network of identified reference objects (red) and additionally image objects of d) are included after shift with dx and dy (green). A determination of rotation angle α is shown. After rotation of the green line the corresponding red marked line of reference is superimposed as well as the shoreline of objects. The determination of the centroid object coordinates, of shift and rotation is described in Fichtelmann and Borg (2015).

A pre-condition for this method is on one side a reference basis like an ortho- or geo-rectified map and on other side identifiable stable landscape objects, like, e.g., lakes. Holm (1991) proposed for the matching of remote sensing data the centers of gravity of patches as ground control points (GCPs). However, it can be that in spite of an available exact geo-referencing basis the geo-referencing of remote sensing data can be difficult or impossible. The reasons for it can be, e.g., that in the case of cloudy scenes the probability of obscuring of usable patches for the geo-correction by clouds is high. However, if the patches can be used, position accuracy in the sub-pixel range in the reference and the image can be achieved. In the case that the pixel resolution of the image with respect to the reference becomes smaller, the probability increases that the GCPs cannot be identified in the image.

Therefore, at least relatively stable landscape objects as e.g. water bodies with relatively well known reflectance characteristics in space and time should be used for the following studies.

At first is assumed that each pixel of map (reference) has the same size as the image pixel allowing an equal-area imaging and topographic effects are not considered. Second, structure information in both data sets must be identified and characterized to link corresponding objects available in remote sensing as well in reference data. In the end, a relation (affine transformation) must be derived between remote sensing and reference data.

In the reference map of our demonstration example (Figure 5a) as well as in the classified image data (Figure 5b) different islands e.g. Ruegen (largest island of Germany, center), Bornholm (Island of Denmark, upper right) are shown as potentially referencing objects.

The processor i) classifies the remote sensing data (water and no-water objects), ii.) eliminates small objects (e.g. < 50 pixels) or having contact to image border (e.g. Bornholm) or clouds, iii) sorts remaining objects based on size, iv) labels them with an identification number (ID), v) determinates shoreline of selected objects, and vi) computes centroids of objects. Additionally a graph network will be constructed automatically using centroids as nodes. Only the network part of directly neighboring objects is marked by blue lines (as crossing-free triangles) in Figure 5c and 5d. The complete data set of graphs is stored in a matrix. The relations of graph network (graph characterized by magnitude and direction) are a characteristic structure which permits the match of constructed graph network of image and reference data.

Further, when using satellite data as segment of a path or using for example classified data based on it as shown in Figure 5b, then a shift from image line to image line has to be calculated. The preparation is necessary because the earth rotates when the satellite is flying over. This assumes that the latitude of corner coordinates of the scene is known within a limit of some pixels. All preliminary pixel coordinates can if not available, calculated on basis of the available corner coordinates, the equations for distances, angles on surface of a sphere and transformations of the spherical coordinate system can be used (Bronstein et al., 2000, 2001). The shift in longitude (caused by rotation) of the nadir point on the small circle of the corresponding geographic latitude can be transformed in a metric distance and at least in a pixel distance which can be used as shift from image line to image line.

In the second experiment a 1400 x 1400 pixel segment of a classified LANDSAT 7 (available in ETM_FAST_L7A format) scene from the 14th August 2000 was used as reference (Figure 6a) and a smaller 1000 x 1000 segment of a classification of a scene from 17th May 2000 was used as image (Figure 6b). On basis of the water bodies of this two images (the larger one is the reference) the same procedure can run as shown in the example before: construction of graph networks based on centroids of usable objects, usable objects are linked with an ID number (the search was limited to 80 image objects), shift and rotation for the affine transformation are determined. Image objects characterized by a threshold of distance to reference object >1 pixel units will be eliminated. For 29 remaining objects of this example the transformation parameters were iterative varied, until the sum of all deviations (distances) has reached a minimum. For example, from the number of remaining objects a Root Mean Square Error ($RMSE_{XY}$) in the order of *0.39 pixel units* can be determined as possible quality measure for allocation.

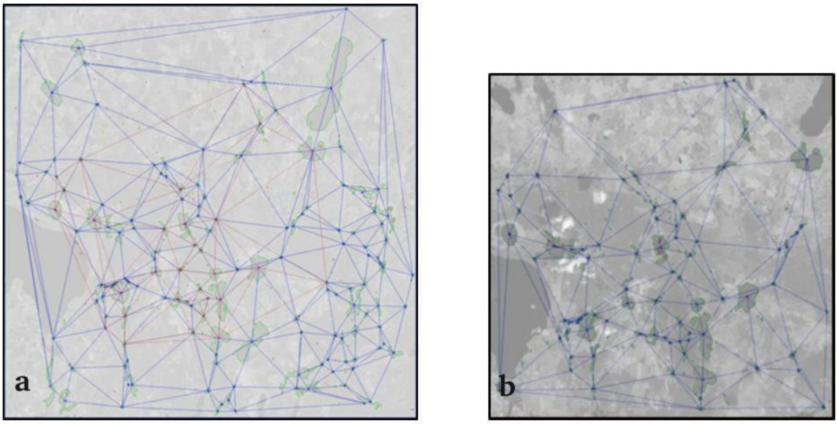

Figure 6: Constructed graph network based on the centroids of identified landscape objects (e.g. water objects-nodes) in reference (left) and image data to be geo-referenced (right) without crossing of graphs showing band 4 data in the background. The contours of usable objects are green marked. The graph network of identified objects with a distance <1 pixel is red marked in the reference (a).

In the third experiment we used the classified water objects and identified islands of 5 LANDSAT 7 scenes of the acquisition period 2000 as images and a map of the corresponding region in the Northeast of Germany with the CIA land-water mask. Figure 7a shows shifts in the overlay of contours of the objects of a section of these five scenes in different colors when using the available geographic coordinates and Figure 7b demonstrates the reduced shifts in the overlay of the same contours after geo-correction using the graph network as described before. In our experiment shifts (in y and y-direction) by 5 pixels could be observed between the different scenes. Further investigations for the determination of the quality are necessary.

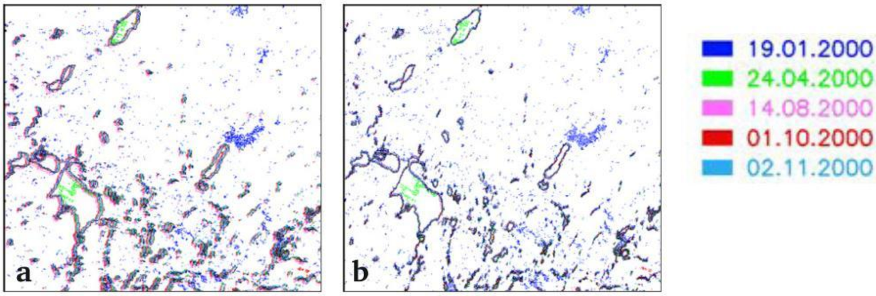

Figure 7: Multi-temporal contours of detected object (regional section of 5 LANDSAT scenes: acquisition period 2000). a) comparison based on corner coordinates, b) based on transformation parameters derived by proposed geo-referencing method.

3.4 Improving pre-processed products by generating dynamic land-water mask

The aim of classification is the assignment of each image pixel to a particular class with very specific properties, in case of vegetation (e.g. in agriculture) with changing specific conditions. In case of clear weather conditions (quality assessment of data) corresponding results can have a very good quality. As one example Hansen et al. (2013a and b) use for their Global Maps of Forest Cover Change more than six hundred thousand Landsat 7 images of growing season. As part of pre-processing a cloud/shadow/ water screening and quality assessment (QA) was performed to get a “stack of QA layers used to create a per-pixel set of cloud-free image observations” and at least time series of global forest cover from 2000 to 2012 (under this perspective a thematic data evaluation including tree cover loss and gain year by year).
For the global forest product only pixel of sufficient quality are used. In case of other products, e.g. burned area detection as part of the ESA-CCI Fire Disturbance Project (ESA) it was necessary on one side to (re)process all MERIS,

(A)ATSR and SPOT-VGT data and on other side to prevent that other dark objects as water or cloud shadow are not included as burned area in the calculations to minimize errors in their detection. But the precise global detection of water bodies itself is a complex task. As already mentioned in Fichtelmann and Borg (2012) and Fichtelmann et al. (2015) remote sensing data are connected with changing atmospheric conditions as haze, aerosol and cloud but also due to the surface roughness of water bodies. Additionally, different components as chlorophyll, yellow substance or suspended sediments influence the spectral characteristics of water bodies, e.g. the continuous decrease of reflectance from the blue to the red part of the spectrum.

The used static land-water masks do not describe the dynamic behavior of the global water body. For that case a Dynamic Self-Learning Evaluation Method (DySLEM) was developed for AATSR (Fichtelmann and Borg, 2012), MERIS-FR(S), MERIS-RR (Fichtelmann et al., 2014), and for SPOT VEGETATION (SPOT-VGT) data (Fichtelmann et al., 2015). The method can be applied on a global scale but the learning algorithm itself is performed on a regional scale by subdividing the input-data set in subsets.

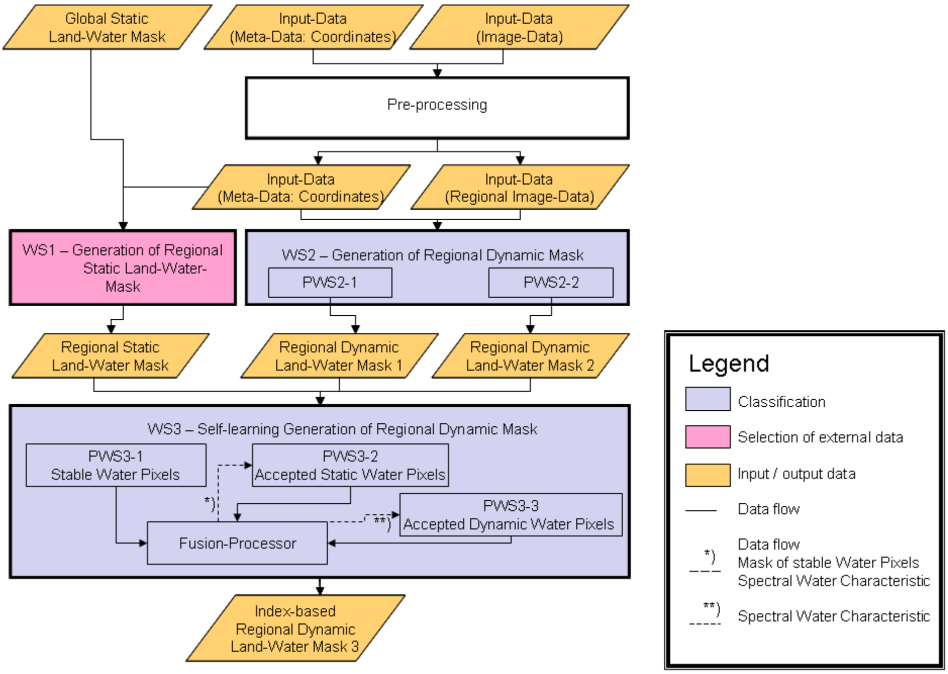

Figure 8: Structure of the processing chain of the DySLEM-processor (Fichtelmann and Borg, 2012).

The operational processing of the dynamic land-water mask includes three processing steps WS as schematic shown in Figure 8.

The working step WS1 generates a regional static land-water mask for the coverage of the input data by using a global static land-water masks as SRTM or/and GSHHS. The result is a raster layer showing the fraction of water area per pixel. All pixels with a fraction of water area above a pre-defined threshold are used later as "static candidates" for water.

The working step WS2 includes two spectral sub-processors for classification of pixels as "dynamic candidates" for water. The aim is to eliminate as many pixels as possible as "non-water" and the result is are two masks of "dynamic candidates" for water.

The task of the third working step WS3 is the fusion of the land-water masks processed in the steps before. The first sub-processor PWS3-1 determines the intersection of the "static" and "dynamic candidates" for water to get "reliable water pixels". Corresponding water pixels are signed in the final mask as "stable water pixels" and excluded from further classification. The sub-processor PWS3-2 uses the mean spectrum of the "stable water pixels" (on regional level, subset of image) to test if the spectra of all remaining pixels are similar to the mean spectrum. In case of similarity within a limit "static candidate" pixels will be accepted and labelled in the resulting mask. All non-accepted static water pixels are excluded from the further processing and not included in the resulting mask. These first two sub-processors may be referred to as quality control of the static mask.

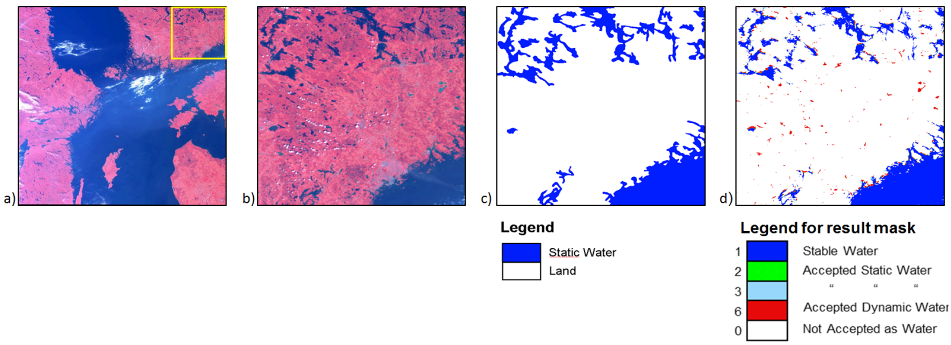

Figure 9: RGB-image (bands 15, 6 and 2) of MERIS-FR(S) data from 14th June 2006 (a) and a subset marked in the upper right (b), static land-water mask based on GSHHS data with ≥10 % fraction of water of image pixel (c) land dynamic land-water mask of the method DySLEM (d).

Pixel candidates which are accepted as water by the processor WS2 and not accepted by sub-processor PWS3-1 will be checked again by the sub-processor PWS3-3. Pixels which are defined by processor PWS3-3 according to spectral features will be masked as "accepted dynamic water" and labelled in the final regional dynamic land-water mask.

In Figure 9 is shown the result of DySLEM for a MERIS-FR(S) subset (Figure 9b) with Finland and Baltic Sea. Figure 9c shows the static land-water mask on basis of the GSHHS static land-water mask. The resulting dynamic land-water mask in Figure 9d shows the dynamic land-water mask, at least the corrected static land-water mask of Figure 9c. The coastline shows more details, additional islands and new water bodies (red marked “accepted dynamic water”) and the shape of many water bodies was changed. Already a simple comparison with the original data shows a much better coincidence of the corresponding water bodies. In other examples DySLEM can identify water bodies below dust and thin clouds (with a little bit lower confidence), corrects a shift of water bodies between static mask and data or correct in the dynamic land-water mask the disappearance of a water body available in the static land-water mask.

4 CONCLUSIONS

The increasing number of available remote sensing missions, sensors, and data, the increasing power of receiving and computation infrastructure, and increasing number of developed automated algorithms, processing chains and value-adding tools for remote sensing data offer the possibility, to fulfil the demands of a regional or global monitoring for environmental as well as security applications.

With respect to the automated processing of optical remote sensing data to value-added information products different pre-processing steps (as e.g. geo-referencing, land-water masking) can be optimized by integrating additional information like land-water masks. But also for the atmosphere correction (a further pre-processing step), the land-water mask can be helpful in a pre-classification step and to identify dark objects used to estimate the aerosol concentration (e.g. Holzer-Popp et al., 2002).

Further operational applications are possible to support value-added processing steps like object identification (e.g. clouds, ice) in optical data or for the identification of burnt surfaces. The classification of these areas can be complicated because soot-blackened objects can have in the visible light a similar appearance as for example cloud shaded areas, water surfaces or mixing pixels with a water land distribution. The identification of water- and land-water-mixing pixel on the basis of land-water masks in the approach of an automatic classification of burnt regions is therefore a possibility to minimize the risk of a false classification of image pixels.

ACKNOWLEDGEMENTS

Dear Hartmut, thank you for your interest in our works all the years and thank you for your kindly support, and the time which we might spend with you by constructive discussions. It was always a pleasure to work together with you. Thank you!

Additional, the developments shown and discussed in our paper ware made possible by Drs. Beruti, Pitella and Biasutti (all of European Space Agency) for the provision of test data, constructive discussions, and interest shown in our investigations. And our results were made possible by ESA CCI ECV Fire Disturbance project (fire_cci), №4000101779/10/I-LG. The authors would like to acknowledge the use of the following free datasets:

USGS for providing the SRTM Water Body Data (SWBD), version 2.1
NOAA National Geophysical Data Center (NGDC) for providing the GSHHS data (A Global Self-consistent, Hierarchical, High-resolution Geography Database).

We thank our retired colleague, Dr. Kurt P. Günther, for fruitful discussions about the design of operational processing chains and for his critical comments.

LITERATURE

BORG, E. (2007): Entwicklung und Anwendung eines automatischen Prozessors zur Erfassung der Wolkenbedeckung und Datennutzbarkeit am Beispiel von LANDSAT 7/ETM+-Daten. Dissertation, Universität Potsdam, Mathematisch-Naturwissenschaftliche Fakultät, Geofernerkundung, Geoinformatik und Kartographie, Potsdam. p. 147.

BORG, E.; FICHTELMANN, B.; ASCHE, H. (2012): Cloud Classification in JPEG-compressed Remote Sensing Data (LANDSAT 7/ETM+). In: B. Murgante et al. (Eds.): 12th International Conference, Salvador de Bahia, Brazil, June 18–21, 2012 Proceedings, Part II, LNCS 7334, Springer, Heidelberg (ISBN 978-3-642-31074-4. ISSN 0302-9743, DOI:10.1007/978-3-642-31075-1_26), pp. 347–357.

BORG, E.; FICHTELMANN, B. AND ASCHE, H. (2013): Data Usability Processor for Optical Remote Sensing Imagery: Design and Implementation into an Automated Processing Chain. In: Murgante, B.; Gervasi, O.; Iglesias, A. Tainar; D. & B. Apduhan, Eds., 13th International conference on computational science and its applications (ICCSA 2013). Lecture Notes in Computer Science. Springer: Berlin-Heidelberg, pp. 635–651.

BORG, E.; FICHTELMANN, B. AND GUENTHER, K. P. (2016): Dynamic self-learning water-masking algorithm for AATSR, MERIS, and SPOT VEGETATION (in press).

BRONSTEIN, I. N.; SEMENDJAJEW, K. A.; MUSIOL, G.; MUELIG, H. (2000, 2001): Taschenbuch der Mathematik, Verlag Harri Deutsch, Thun u. Frankfurt a. M.

BROWN, L. G. (1992): A survey of image registration techniques. ACM Computing Surveys, 24, 4, pp. 325–376.

CARROLL, M. L.; TOWNSHEND, J. R.; DIMICELI, C. M.; NOOJIPADY, P. AND SOHLBERG, R. A. (2009): A new global raster water mask at 250 m resolution, Int. J. of Digital Earth, Vol. 2, No. 4, pp. 291–308.

FEISTEL, R. (1999): New shoreline map-drawing data available, Eos Trans. AGU, Vol. 80, No. 22, p. 249, DOI:10.1029/99EO00188.

FENG, M.; SEXTON, J. O.; CHANNAN, S. AND TOWNSHEND, J. R. (2015): A global, high-resolution (30 m) inland water body dataset for 2000: first results of a topographic–spectral classification algorithm, Int. J. of Digital Earth, Vol. 9, No. 2, pp. 1–21.

FICHTELMANN, B.; BORG, E.; GÜNTHER, A.; GUDER, H.-G., REIMER, R.; WOLFF, E., DAMEROW, H. (2001): Chlorophyll Map of the Baltic Sea – The Results of an automatic processing chain from data reception up to archiving and delivery of value-added products. Abstract Book (Eds. Bruzzone, L.; Smith, P.), European Commission – Joint Research Centre – Special Publications I.01.122, p. 50.

FICHTELMANN, B.; BORG, E. AND KRIEGEL, M. (2011): Verfahren zur operationellen Bereitstellung von Zusatzdaten für die automatische Fernerkundungsdatenverarbeitung, Angewandte Geoinformatik 2011, (Eds.: Strobl, Blaschke, Griesebner), 23. AGIT Symposium, Salzburg, pp. 12–20.

FICHTELMANN, B.; BORG, E. AND GUENTHER, K. P. (2014): Adaption of a Self-learning Algorithm for Dynamic Classification of Water Bodies to MERIS Data, Proceedings of Computational Science and its Applications, ICCSA 2014, Part I, LNCS 8579, Springer International Publishing Switzerland 2014, pp. 376–392.

FICHTELMANN, B. AND BORG, E. (2012): A new Self-learning Algorithm for Dynamic Classification of Water Bodies, Proceedings of Computational Science and its Applications – ICCSA 2012, Part III, LNCS 7335, Springer-Verlag Berlin Heidelberg 2012, pp. 457–470.

FICHTELMANN, B. AND BORG, E. (2015): A new approach of geo-rectification for time series satellite data based on a graph-network, Proceedings of Computational Science and its Applications – ICCSA 2015, Part IV, LNCS 9158, Springer International Publishing Switzerland 2015, pp. 217–232.

FICHTELMANN, B.; GUENTHER, K. P. AND BORG, E. (2015): Adaption of a Self-Learning Algorithm for Dynamic Classification of Water Bodies to SPOT VEGETATION Data, Proceedings of Computational Science and its Applications – ICCSA 2015, Part IV, LNCS 9158, Springer International Publishing Switzerland 2015, pp. 177–192.

GMES:http://www.eurogeographics.org/sites/default/files/imported-files/documents/GMES_Newsletter_1.pdf.

GUENTHER, K. P.; NEUMANN, A.; GEGE, P.; DOERFFER, R.; FISCHER, J.; BROCKMANN, C.: (2002) MERIS – Value added – products for land-, water and atmospheric applications. In: Tagungsband 19. DFD-Nutzerseminar, 15.–16. Oktober 2002, S. Dech et al. (EDS.), pp. 37–51, 2002.

GUENTHER, K. P.; KRAUSS, T.; RICHTER, R.; MÜLLER, R.; FICHTELMANN, B.; BORG, E.; BACHMANN, M.; WURM, M.; GSTAIGER, V. AND MÜLLER, A.: (2012): Operational pre-processing of MERIS, (A)ATSR and VEGETATION data for the ESA-CCI project "Fire-Disturbance", EGU General Assembly, 22.–27. April 2012, Vienna, Austria.

HANSEN, M. C.; POTAPOV, P. V.; MOORE, R.; HANCHER, M.; TURUBANOVA, S. A.; TYUKAVINA, A.; THAU, D.; STEHMAN, S. V.; GOETZ, S. J.; LOVELAND, T. R.; KOMMAREDDY, A.; EGOROV, A.; CHINI, L.; JUSTICE, C. O. AND TOWNSHEND, J. R. G. (2013a): High-Resolution Global Maps of 21st-Century Forest Cover Change, Science, Vol. 342, pp. 850–853.

HANSEN, M. C.; POTAPOV, P. V.; MOORE, R.; HANCHER, M.; TURUBANOVA, S. A.; TYUKAVINA, A.; THAU, D.; STEHMAN, S. V.; GOETZ, S. J.; LOVELAND, T. R.; KOMMAREDDY, A.; EGOROV, A.; CHINI, L.; JUSTICE, C. O. AND TOWNSHEND, J. R. G. (2013b): Supplementary Materials for 'High-Resolution Global Maps of 21st-Century Forest Cover Change', http://sciencemag.org/content/342/6160/850/suppl/DC1 (Accessed 11. October 2016).

HOLM, M.; Towards automatic rectification of satellite images using feature based matching IEEE Xplore, pp. 2439–2442. (http://ieeexplore.ieee.org/stamp/stamp.jsp?arnumber=575537)

HOLZER-POPP, T.; BITTNER, M.; BORG, E.; DECH, S.; ERBERTSEDER, T.; FICHTELMANN, B.; SCHROEDTER, M. (2002): Process for correcting atmospheric influences in multispectral optical remote sensing. UP 6,484,099 B1.

KRAWCZYK, H.; NEUMANN, A.; WALZEL, TH.; HETSCHER, M. AND SIEGEL, H. (1996): Application of a multispectral interpretation algorithm to remote sensing data over the Baltic Sea, SPIE 2963, pp. 234–239.

LEHNER, B. AND DOELL, P. (2004): Development and validation of a global database of lakes, reservoirs, and wetlands, Journal of Hydrology, Vol. 296, pp. 1–22.

LI, M. (1988): High Precision Relative Orientation Using the Feature Based Matching Techniques, Intemational Archives for photogrammetry and Remote Sensing Kyoto, 1988, Vol. 27, commission 111, pp. 456–465.

NEUMANN, A.; KRAWCZYK, H.; BORG, E.; FICHTELMANN, B. (2004): Towards Operational Monitoring of the Baltic Sea by Remote Sensing. In: Managing the Baltic Sea, (EDS. Schernewski, G. & Löser, N.) Coastline Reports, 2, EUCC, pp. 211–218.

PADILLA, M.; OLIVA, P. AND CHUVIECO, E. (2012): ESA CCI ECV Fire Disturbance (fire_cci) (1012), N° 4000101779/10/I-LG.

PAPE, D. (last modified 2004): CIA World DataBank II, http://www.evl.uic.edu/pape/data/WDB/ (Accessed 04. October 2016).

SAXENA, S.; SINGH, R. K. (2014): A survey of recent and classical image registration methods. International Journal of Signal Processing, Image Processing and Pattern Recognition. 7, 4, pp. 167–176.

TOUTIN, T. (2004): Geometric processing of remote sensing images: Models, algorithms and methods. Int. J. Remote Sensing, 25, 10, pp. 1893–1924.

USGS (2003): Documentation for the Shuttle Radar Topography Mission (SRTM) Water Body Data Files, http://dds.cr.usgs.gov/srtm/version2_1/SWBD/SWBD_Documentation/Readme_SRTM_Water_Body_Data.pdf (Accessed 04. October 2016).

WESSEL, P. AND SMITH, W. H. F. (1996): A global, self-consistent, hierarchical, high-resolution shoreline database, J. Geophys. Res., Vol. 101 (B4), pp. 8741–8743.

WOLFF, E.; REIMER, R.; BORG, E.; GÜNTHER, A.; BARUTH, B.; FICHTELMANN, B.; PREUSS, H. (1998): Bereitstellung einer operationellen Chlorophyllkarte für die Ostsee, ZPF, Vol. 66, No. 5–6, pp. 146–156, 1998.

ZITOVA, B., J. FLUSSER, J. (2003): Image registration methods: A survey, Image and Vision Computing, Vol. 21, pp. 977–1000.